

## Internal waves in a circular channel

By W. H. YANG AND CHIA-SHUN YIH

Department of Applied Mechanics and Engineering Science,  
University of Michigan, Ann Arbor

(Received 29 May 1975)

The frequencies of the first four sloshing internal wave modes in two superposed fluid layers contained in a circular channel are calculated for two positions of the free surface and for various ratios of the depths of the two layers. Flow patterns are given for the first four sloshing modes for the case in which the fluids occupy a semicircular space and the depth of the upper layer is one-quarter of the radius.

It is hoped that the results obtained will provide a guide for estimating the frequencies of sloshing internal wave modes in long lakes.

---

### 1. Introduction

It is well known that exact solutions for water waves in channels of variable depth are extremely few (Lamb 1932, pp. 442–450). For internal waves in superposed layers each of uniform density, no exact solutions are known if the depth of the container is not uniform except the edge-wave solutions given by Yih (1965, p. 57; 1966).

Internal waves occupy an important position in limnology, since lakes are thermally stratified most of the time. Limnologists generally use a model consisting of two superposed layers, each homogeneous in itself, to approximate the actual distribution of temperature and density. But, as stated above, non-uniformity of depth always presents difficulties surmountable only by resorting to numerical computations.

In order to provide some guide for limnologists we have carried out calculations of the frequencies of the first four sloshing internal wave modes in two superposed fluid layers in a circular channel (see figure 1) for different ratios of the depths of the layers and for two positions of the free surface. Also, the flow patterns for the first four sloshing modes are given for the case when the fluids occupy a semicircular space and the depth of the upper layer is one-quarter of the radius of the channel.

The frequencies for the cases of an extremely shallow upper or lower layer have been obtained analytically by adapting the solutions of Budiansky (1960) for a homogeneous fluid to the present case. All the other calculations are numerical ones carried out by replacing the differential system governing internal waves by linear algebraic equations.

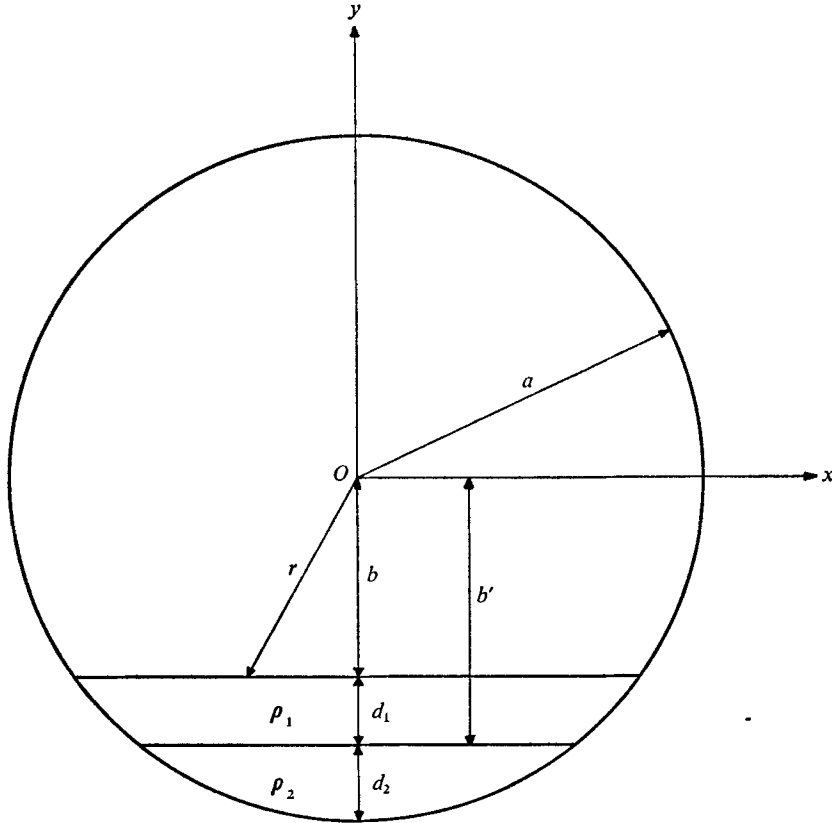


FIGURE 1. Definition sketch.

**2. The differential system**

We shall denote the density of the upper fluid by  $\rho_1$  and that of the lower fluid by  $\rho_2$ . Since each layer is homogeneous, we shall assume the flow in each layer to be irrotational, and denote the velocity potential for the upper layer by  $\phi_1$  and that for the lower layer by  $\phi_2$ .

Then

$$\nabla^2\phi_1 = 0, \quad \nabla^2\phi_2 = 0, \tag{1}$$

where

$$\nabla^2 = \partial^2/\partial x^2 + \partial^2/\partial y^2,$$

$x$  and  $y$  being Cartesian co-ordinates, with  $y$  measured in the vertical direction. The condition at the solid boundary of the channel is, for either layer,

$$\partial\phi/\partial n = 0, \tag{2}$$

where  $n$  is measured in a direction normal to the boundary.

At the free surface the pressure is constant. By combining the kinematic condition with the Bernoulli equation we get the free-surface condition

$$\partial^2\phi_1/\partial t^2 + g\partial\phi_1/\partial y = 0.$$

If we assume the exponential factor  $\exp(-i\sigma t)$  for all perturbation quantities, this condition becomes

$$\sigma^2 \phi_1 = g \phi_{1y}, \quad (3)$$

in which the subscripts  $t$  and  $y$  indicate partial differentiation.

On the interface the kinematic condition is

$$\phi_{1y} = \phi_{2y} \quad (4)$$

and the dynamic condition, obtained in a similar way to (3), is

$$\sigma^2(\rho_2 \phi_2 - \rho_1 \phi_1) = g(\rho_2 - \rho_1) \phi_{1y}. \quad (5)$$

The differential system to be solved consists of (1)–(5), with  $\sigma^2$  as the eigenvalue.

In our numerical calculations it is often convenient to use stream functions. In terms of the stream functions  $\psi_1$  and  $\psi_2$ , with the subscript 1 indicating the upper layer and the subscript 2 indicating the lower layer, the differential system consists of the following equations:

$$\nabla^2 \psi_1 = 0, \quad \nabla^2 \psi_2 = 0, \quad (6)$$

$$\psi_1 = 0 = \psi_2 \quad \text{on the solid boundary,} \quad (7)$$

$$\sigma^2 \psi_{1y} = g \psi_{1yy} \quad \text{on the free surface,} \quad (8)$$

$$\psi_1 = \psi_2 \quad \text{on the interface,} \quad (9)$$

$$\sigma^2(\rho_2 \psi_2 - \rho_1 \psi_1)_y = g(\rho_2 - \rho_1) \psi_{1yy} \quad \text{on the interface.} \quad (10)$$

Conditions (8) and (10) are obtained by differentiating (3) and (5) with respect to  $x$  and using the Cauchy–Riemann equations, and (9) follows directly from (4) on using the Cauchy–Riemann equations.

### 3. Asymptotic solutions for the special cases in which one layer is extremely thin

We shall give some exact results for the extreme cases in which either the upper layer or the lower layer is exceedingly thin, which cannot be conveniently solved by numerical computation. These results will provide some check on the trend of the numerical results and some guidance as to the curves representing them. For internal waves the free surface can be considered fixed.

For the case of an extremely thin upper layer, when the maximum total depth is fixed, the result is simply that for *internal waves*

$$\sigma = 0.$$

The reasoning is briefly as follows. Compare the case with the case of internal waves in a rectangular channel with the total depth equal to the maximum total depth in the circular channel, the upper-layer depth exactly equal to that for the case under consideration and the width equal to the width of the interface.

The  $\sigma$  for the circular channel can be shown to be less (Yih 1975) than that for the rectangular channel, for the interfaces are of the same width, the excess area occupied by the thin upper fluid in the circular channel over that in the rectangular channel is negligibly small, whereas the domain of the lower fluid in the rectangular channel contains that in the circular channel. For *internal* waves in the rectangular channel the upper surface can be taken as flat, and the frequency is given, after a simple calculation using (1), (2), (4) and (5), by

$$\sigma^2 = g'_1 \tanh k d_1,$$

where  $d_1$  is the depth of the upper fluid,

$$g'_1 = (\Delta\rho/\rho_1)g, \quad \Delta\rho = \rho_2 - \rho_1$$

and

$$k = (2n + 1)\pi/b \quad \text{or} \quad 2n\pi/b,$$

$b$  being the width of the rectangular channel and  $n$  a positive integer. It is clear then that the  $\sigma$  for the rectangular channel approaches zero as  $d_1$  approaches zero, and *a fortiori* the  $\sigma$  for the circular channel must approach zero. This calculation also illustrates the well-known fact that when either layer is thin we can replace  $g$  by  $g\Delta\rho/\rho$  for the thin layer, and ignore the existence of the deep layer. This fact will be recalled when we calculate  $\sigma$  for the case of a thin lower layer in the following paragraphs.

For the case of an extremely thin lower layer, we note first that, as has been mentioned, when the lower layer is very thin the frequency of any internal wave mode is the same as that of the corresponding free-surface wave mode for a single layer (the thin lower layer), as though the upper fluid did not exist, if  $g$  is changed to

$$g' = \frac{\rho_2 - \rho_1}{\rho_2} g. \quad (11)$$

Thus to find the  $\sigma$  for the case of a very thin lower layer, we need to find only the  $\sigma$  for free-surface waves on that layer, but with  $g$  replaced by  $g'$ .

For the first sloshing mode, we take

$$\phi_2 = \theta = -\arctan(x/y),$$

which satisfies (11) and (12). On the free surface, where  $y = -b'$ , we have, after some simple calculations and using (3), with  $\phi_2$  replacing  $\phi_1$ ,

$$\sigma^2 = g'/b',$$

if terms  $O[(x/b')^3]$  are neglected. Note that  $x'/b$  is small if the lower layer is thin, or  $a - b' \ll a =$  radius of circular channel. In the limit,

$$\sigma^2 = g'/a. \quad (12)$$

Solutions for higher modes can be obtained similarly. But the solutions for the modes can also all be obtained at once by adapting Budiansky's solutions

for a single thin layer, by merely replacing his  $g$  by our  $g'$ . The long-wave equation used by Budiansky becomes, after replacement of  $\phi_2$  by  $\phi$  and  $g$  by  $g'$ ,

$$\frac{\partial}{\partial x} (h_2 \phi_x) + \frac{\sigma^2}{g'} \phi = 0, \quad (13)$$

where  $h_2 = (a^2 - x^2)^{\frac{1}{2}} - b' \doteq (a - b') - x^2/2a$ .

With  $\xi^2 = 2a(a - b')x^2$ , (13) can be written as

$$\frac{\partial}{\partial \xi} [(1 - \xi^2) \phi_\xi] + \frac{2a\sigma^2}{g'} \phi = 0, \quad (14)$$

which is Legendre's equation. In order not to have any singularities at  $\xi^2 = 1$ , it is necessary that

$$2\sigma^2 a/g' = n(n+1), \quad (15)$$

$n$  being an integer representing the mode. For  $n = 1$ , (15) gives (12), as expected.

#### 4. Algebraic method for the numerical solutions

When the differential system (1)–(5) is discretized by either a finite-difference or a finite-element method, it reduces to an algebraic eigenvalue problem approximating the original equations, but not the standard algebraic eigenvalue problem

$$\mathbf{A}\mathbf{x} = \lambda\mathbf{x}. \quad (16)$$

It is possible to reduce the differential system only to

$$\mathbf{A}\mathbf{x} = \lambda\mathbf{B}\mathbf{x}, \quad (17)$$

where  $\mathbf{A}$  and  $\mathbf{B}$  are constant matrices and  $\lambda$  and  $\mathbf{x}$  denote the eigenvalues and eigenvectors, respectively. When the variables on the free surface and interface are eliminated, the algebraic eigenvalue problem takes the form

$$\mathbf{N}(\lambda)\mathbf{x} = 0, \quad (18)$$

where the eigenvalue  $\lambda$  appears nonlinearly in the elements of the matrix  $\mathbf{N}$ . The dimension of  $\mathbf{N}$  is smaller than that of  $\mathbf{A}$ . Such an eigenvalue problem has been studied recently (Kublanovskaya 1970). Efficient algorithms are just being developed for its solution.

For the algebraic formulation, subscripts are reserved for vector and matrix components. We shall denote the velocity potential in the domain  $D_1$  of the lighter fluid by  $\phi^{(1)}(x, y, t)$  and that in the domain  $D_2$  of the heavier fluid by  $\phi^{(2)}(x, y, t)$ . For convenience in a parametric analysis for the various locations of the interface to be considered in this study, a regular grid with a constant mesh is most desirable. As a result, the finite-difference method with a constant mesh size  $H$  is used, with linear interpolation for the curved boundaries.

Let  $\phi_F^{(1)}$ , a vector, be the projection of the potential function on the free surface in the approximating finite-dimensional space and  $\phi_1^{(1)}, \phi_2^{(1)}, \dots, \phi_m^{(1)}$  be the vector representations of the potential function in  $D_1$  at consecutive levels of the grid downwards from the free surface. Let  $\phi_I^{(1)}$  and  $\phi_I^{(2)}$  represent the potential

functions on the interface, and  $\phi_1^{(2)}, \phi_2^{(2)}, \dots, \phi_n^{(2)}$  represent the potential function in  $D_2$  at consecutive grid levels downwards from the interface. With the condition at the container's boundary taken into consideration, the algebraic system of equations approximating (1) and (2) may be written in the matrix form

$$\begin{bmatrix} \mathbf{A}_F & \mathbf{A}_{11} & \mathbf{A}_{12} \\ & \mathbf{A}_{21} & \mathbf{A}_{22} & \mathbf{A}_{23} \\ & & \dots & \dots & \dots \\ & & & \mathbf{A}_{m,m-1} & \mathbf{A}_{m,m} & \mathbf{A}_I \\ & & & & \mathbf{B}_I & \mathbf{B}_{11} & \mathbf{B}_{12} \\ & & & & & \mathbf{B}_{21} & \mathbf{B}_{22} & \mathbf{B}_{23} \\ & & & & & & \dots & \dots & \dots \\ & & & & & & & & \mathbf{B}_{n,n-1} & \mathbf{B}_{n,n} \end{bmatrix} \begin{pmatrix} \phi_F^{(1)} \\ \phi_1^{(1)} \\ \vdots \\ \phi_m^{(1)} \\ \phi_I^{(1)} \\ \phi_I^{(2)} \\ \phi_1^{(2)} \\ \vdots \\ \phi_n^{(2)} \end{pmatrix} = 0, \quad (19)$$

where the  $\mathbf{A}$ 's and  $\mathbf{B}$ 's with different subscripts are constant matrices of dimensions compatible with that of the  $\phi$ 's, and the blanks in the global matrix denote zero entries.

The approximate algebraic form of the free-surface condition (3) is

$$\phi_F^{(1)} = (1 - \lambda)^{-1} \phi_I^{(1)}, \quad (20)$$

where

$$\lambda = (H/g)\sigma^2.$$

The interface continuity conditions (4) and (5) can be reduced to

$$\begin{pmatrix} \phi_I^{(1)} \\ \phi_I^{(2)} \end{pmatrix} = \frac{1}{\lambda\delta(1+\gamma)-1} \begin{bmatrix} \lambda\delta\gamma-1 & \lambda\delta\gamma \\ \lambda\delta & \lambda\delta-1 \end{bmatrix} \begin{pmatrix} \phi_m^{(1)} \\ \phi_1^{(2)} \end{pmatrix}, \quad (21)$$

where

$$\delta = \rho_1/(\rho_2 - \rho_1), \quad \gamma = \rho_2/\rho_1.$$

After the use of (20) and (21) the matrix equation (19) can be rearranged to give

$$\begin{bmatrix} \mathbf{A}'_{11} & & & & & & & & & \\ & \mathbf{A}_{12} & & & & & & & & \\ & \mathbf{A}_{21} & \mathbf{A}_{22} & \mathbf{A}_{23} & & & & & & \\ & & \dots & \dots & \dots & & & & & \\ & & & & \mathbf{A}_{m,m-1} & (\mathbf{A}_{m,m} + g_1 \mathbf{A}_I) & g_2 \mathbf{A}_I & & & \\ & & & & & g_3 \mathbf{B}_I & (\mathbf{B}_{11} + g_4 \mathbf{B}_I) & \mathbf{B}_{12} & & \\ & & & & & & \dots & \dots & \dots & \\ & & & & & & & & & \mathbf{B}_{n,n-1} \mathbf{B}_{n,n} \end{bmatrix} \begin{pmatrix} \phi_1^{(1)} \\ \vdots \\ \phi_m^{(1)} \\ \phi_1^{(2)} \\ \vdots \\ \phi_n^{(2)} \end{pmatrix} = 0, \quad (22)$$

where  $g_1, g_2, g_3$  and  $g_4$  are functions of  $\lambda$ :

$$\left. \begin{aligned} g_1(\lambda) &= (\lambda\delta\gamma - 1)/g(\lambda), \quad g_2(\lambda) = \lambda\delta\gamma/g(\lambda), \\ g_3(\lambda) &= \lambda\delta/g(\lambda), \quad g_4(\lambda) = (\lambda\delta - 1)/g(\lambda), \\ g(\lambda) &= (1 + \gamma)\lambda\delta - 1, \quad \mathbf{A}'_{11} = \mathbf{A}_{11} + (1 + \lambda)^{-1} \mathbf{A}_F. \end{aligned} \right\} \quad (23)$$

Equation (22) has the form of the general eigenvalue problem given in (18). We shall thus write (22) in the compact notation

$$\mathbf{N}(\lambda)\phi = 0. \quad (24)$$

This equation is solved by an iterative method (Yang 1975). For a given estimate of the eigenvalue  $\lambda$ , we seek an improvement  $\mu = \Delta\lambda$  satisfying

$$\det(\mathbf{N}(\lambda + \mu)) = 0. \tag{25}$$

$\mu$  is obviously a function of  $\lambda$ . This function can be expressed as

$$\mu(\lambda) = -(\text{tr}(\mathbf{L}^{-1}\mathbf{P}\mathbf{N}'\mathbf{U}^{-1}))^{-1}, \tag{26}$$

where the matrices  $\mathbf{P}$ ,  $\mathbf{L}$  and  $\mathbf{U}$  are permutation, lower-triangular and upper-triangular matrices, respectively. They are the  $\mathbf{LU}$  decomposition (Forsythe & Moler 1967, p. 36) of  $\mathbf{N}(\lambda)$  such that  $\mathbf{N}(\lambda) = \mathbf{P}^T\mathbf{L}\mathbf{U}$  and

$$\mathbf{N}'(\lambda) = d\mathbf{N}(\lambda)/d\lambda.$$

$\text{tr}(\ )$  denotes the trace of a matrix.

The improved estimate of the eigenvalue is given by

$$\lambda_{k+1} = \lambda_k + \mu(\lambda_k), \quad k = 0, 1, 2, \dots \tag{27}$$

The condition for and properties of convergence of this iteration procedure are known (Yang 1975).

We are interested in only the first (smallest) few eigenvalues. The first four eigenvalues and the associated eigenvectors were calculated and plotted in the form of contours of equal potential and the orthogonal set of streamlines. The streamlines were calculated from the Cauchy–Riemann conditions. A more accurate solution for the streamlines may be obtained from the formulation in terms of the stream function. The equi-potentials and streamlines for the first four modes are shown in figures 2(a)–(d).

It is noted that, for all four modes, the free-surface velocity is nearly horizontal. The largest amplitudes of the waves as well as the kinetic energy are concentrated about the interface. Since the amplitude of surface waves is small for low frequencies, we may approximate the free surface by a rigid surface. Such an approximation further simplifies the algebraic equation (19). Now, only the equations involving the interface contain the eigenvalue. If the stream function is used in the formulation, the differential system (6)–(10) reduces to the approximate algebraic representation

$$\begin{bmatrix}
 \mathbf{C}_{11} & \mathbf{C}_{12} & & & & & & & & & \\
 \mathbf{C}_{21} & \mathbf{C}_{22} & \mathbf{C}_{23} & & & & & & & & \\
 & \dots & \dots & \dots & & & & & & & \\
 & & & & \mathbf{C}_{m,m-1} & \mathbf{C}_{m,m} & \mathbf{C}_I & & & & \\
 & & & & & & \mathbf{D}_I & \mathbf{D}_{11} & \mathbf{D}_{12} & & \\
 & & & & & & & \mathbf{D}_{21} & \mathbf{D}_{22} & \mathbf{D}_{23} & \\
 & & & & & & & & \dots & \dots & \dots \\
 & & & & & & & & & & \mathbf{D}_{n,n-1} & \mathbf{D}_{n,n}
 \end{bmatrix}
 \begin{pmatrix}
 \psi_I^{(1)} \\
 \vdots \\
 \psi_m^{(1)} \\
 \psi_I \\
 \psi_I^{(2)} \\
 \vdots \\
 \psi_n^{(2)}
 \end{pmatrix} = 0, \tag{28}$$

where the  $\mathbf{C}$ 's and  $\mathbf{D}$ 's are constant matrices and  $\psi_{11}^{(1)}, \dots, \psi_m^{(1)}$  are vectors representing the stream function at different levels of the finite-difference grid in the domain  $D_1$ .  $\psi_I$  approximates the interface stream function and  $\psi_I^{(2)}, \dots, \psi_n^{(2)}$  represent the stream function in the domain  $D_2$ .

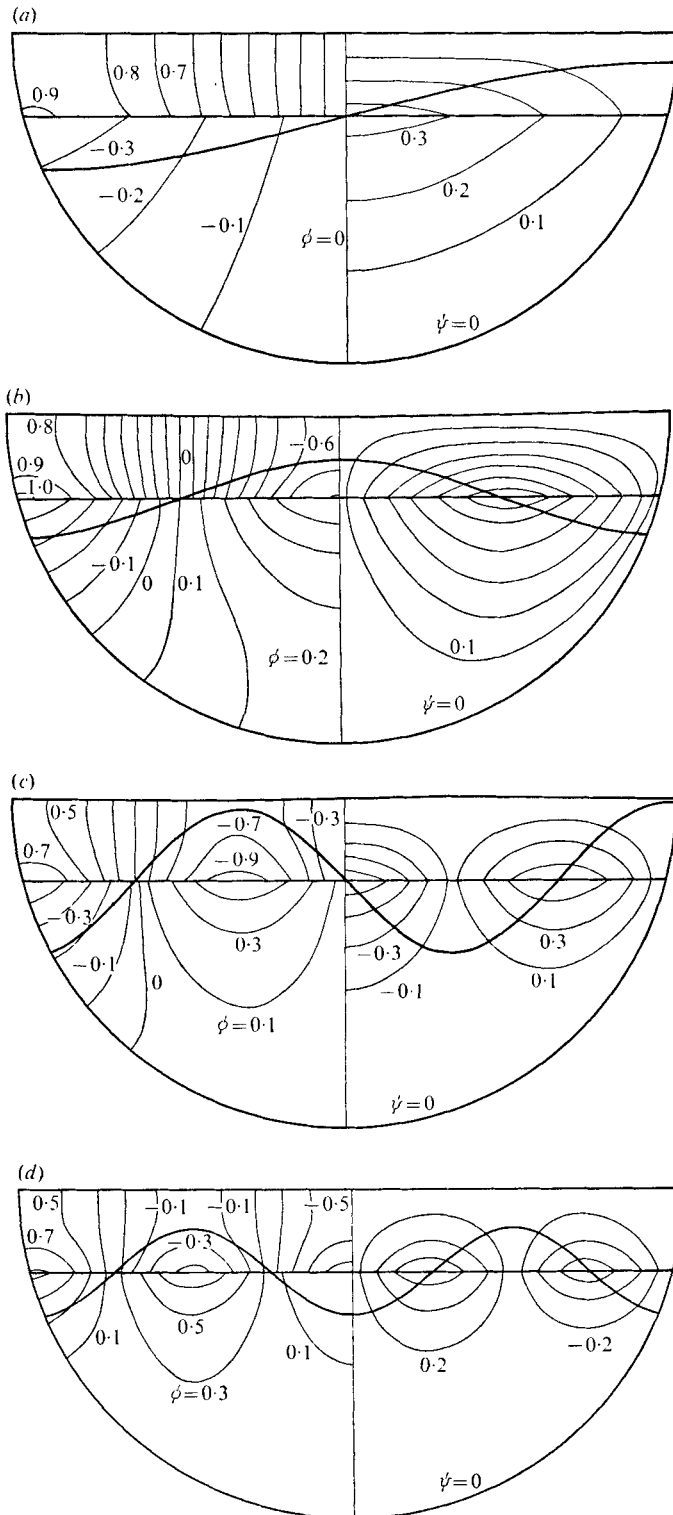


FIGURE 2. Flow patterns for the first four sloshing internal wave modes. The free surface is not assumed flat. The height of the interface is exaggerated. (a) First mode,  $\sigma^2 a/g = 0.0152$ ; contour intervals for the stream function  $\psi$  and velocity potential  $\phi$  0.1 throughout. (b) Second mode,  $\sigma^2 a/g = 0.0465$ ; contour intervals 0.1. (c) Third mode,  $\sigma^2 a/g = 0.794$ ; contour intervals 0.2. (d) Fourth mode,  $\sigma^2 a/g = 0.10843$ ; contour intervals 0.2.



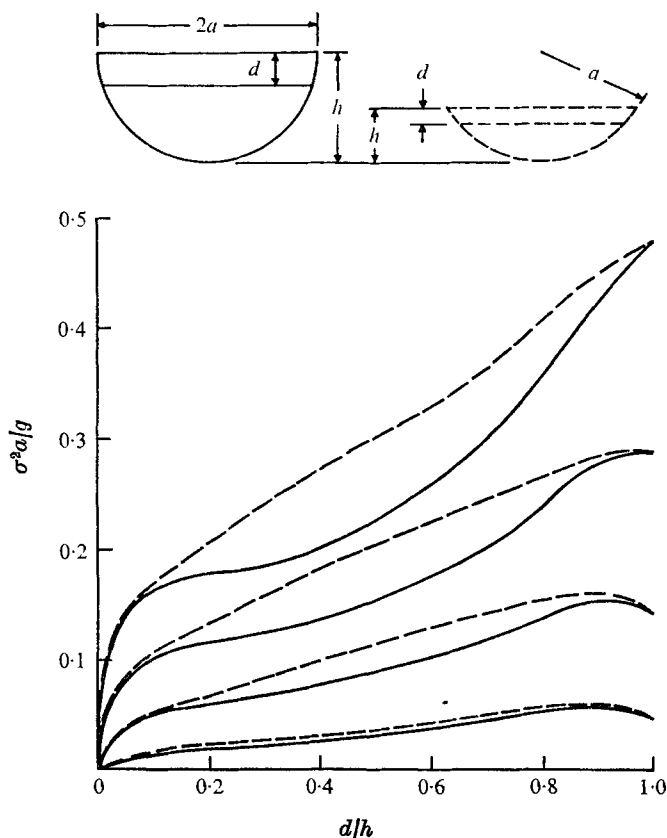


FIGURE 3. Results for  $\sigma^2 a/g$  as a function of  $d/h$ .  
 —,  $h = a$ ; ---,  $2h = a$ .

Since the matrix equation (48) is block-tridiagonal and homogeneous, we may express  $\Psi_1^{(1)}$  in terms of  $\Psi_2^{(1)}$ ,  $\Psi_2^{(1)}$  in terms of  $\Psi_3^{(1)}$ , etc. Thus all the

$$\Psi_i^{(1)} \quad (i = 1, 2, \dots, m)$$

may be expressed in terms of  $\Psi_I$ . Similarly,  $\Psi_n^{(2)}$  may be expressed in terms of  $\Psi_{n-1}^{(2)}$ ,  $\Psi_{n-1}^{(2)}$  in terms of  $\Psi_{n-2}^{(2)}$ , etc. Thus all the  $\Psi_i^{(2)}$  ( $i = n, n-1, \dots, 1$ ) may also be expressed in terms of  $\Psi_I$ .

Finite-difference approximation of the interface conditions (9) and (10) leads to

$$\mathbf{E}\psi_I = \lambda[\gamma(\Psi_I - \Psi_1^{(2)}) - (\Psi_m^{(1)} - \Psi_I)], \tag{29}$$

where  $\mathbf{E}$  is a constant matrix.

Since both  $\Psi_1^{(2)}$  and  $\Psi_m^{(1)}$  may be expressed in terms of  $\Psi_I$ , a single matrix equation with the dimensions of  $\Psi_I$  can be written down:

$$\mathbf{E}\Psi_I = \lambda\mathbf{F}\Psi_I, \tag{30}$$

where  $\mathbf{F}$  is a composite matrix made up of the  $\mathbf{C}$ 's and  $\mathbf{D}$ 's.

The advantage of this approximate formulation is obvious. It involves small dimensions and a standard form of algebraic eigenvalue problem for which efficient subroutines are readily available in every major computing centre. As expected, the solutions differ little from those of the original problem with a free surface at low frequencies. The economy provided by this approximation enabled an extended parametric analysis for various depth ratios of the two layers. The program developed here should be a very efficient tool for studying internal waves in superposed liquid layers in arbitrarily shaped containers. The frequencies of the first four modes for a circular container for various ratios of the depths of the two layers are presented in figure 3 for two positions of the free surface.

## 5. Results

As mentioned before, we have considered the cases  $h = a$  and  $h = \frac{1}{2}a$ , with  $\rho_2/\rho_1 = 1.05$ . For each case the numerical calculation was carried out for several values of  $d/h$  from 0.10 to 0.90. The values of  $\sigma^2 a/g$  are shown in figure 3, in which the curves were extrapolated from zero to 0.10 and from 0.90 to 1.00.

We note that, if the Boussinesq approximation is used, approximate values of  $\sigma^2 a/g$  for other density ratios can be obtained from figure 3 by multiplying the values given therein by  $21(\rho_2 - \rho_1)/\rho_2$ .

We note that for the first sloshing mode  $\sigma^2 a/g$  varies but little with  $h/a$ .

This work has been jointly supported by the National Science Foundation and the Office of Naval Research.

## REFERENCES

- BUDIANSKY, B. 1960 Sloshing of liquids in circular canals and spherical tanks. *J. Aerospace Sci.* **27**, 161–173.
- FORSYTHE, G. & MOLER, C. B. 1967 *Computer Solution of Linear Algebraic Systems*. Prentice-Hall.
- KUBLANOVSKAYA, V. N. 1970 *SIAM J. Numer. Anal.* **7**, no. 4, 1970.
- LAMB, H. 1932 *Hydrodynamics*, 6th edn. Cambridge University Press.
- YANG, W. H. 1975 A method for eigenvalues of  $\lambda$ -matrices. *University of Michigan, AMES Rep.* no. 1702.
- YIH, C.-S. 1965 *Dynamics of Nonhomogeneous Fluids*. Macmillan.
- YIH, C.-S. 1966 Note on edge waves in a stratified fluid. *J. Fluid Mech.* **24**, 765–767.
- YIH, C.-S. 1975 Comparison theorems for water waves in basins of variable depth. *Quart. Appl. Math.* To be published.